

Converted wave processing in the EOM domain

Thais A. Guirigay and John C. Bancroft

ABSTRACT

A new approach for converted wave prestack migration and velocity analysis has been developed. That is based on the consideration of prestack migration by equivalent offset and common scatter points (CSP). During the process, a converted wave velocity V_c was estimated from the hyperbolic moveout on a CSP gathers. Moveout (MO) correction and stacking complete the prestack migration. The intent of this paper is to see what additional uses can be made with V_c .

Converted wave CSP gathers are formed by summing all input traces at the equivalent offset migration. A limited converted wave CSP (LCCSP) gather can be formed if we assume V_c replace V_p and V_s . V_c is valid only for zero offset data, however we can extend its application when there is an acceptable small error in the estimated traveltimes.

For a given trace with an acceptable time error, there may be still considerable trace energy to form a reasonable LCCSP.

INTRODUCTION

Reflection seismic exploration has been concerned predominately with P-wave energy for many reasons that include: compressional waves arrive first, they have high signal-to-noise ratios, usually particle motion that is close to rectilinear, are easily generated by a variety of sources, and propagate in fluid. Because many basins are or will be soon in mature stage, we need the development of new technologies, and converted shear wave seismic exploration is one of them. Converted wave exploration refers to a downward-propagating P-wave, converting on reflection at its deepest point of penetration to an upward-propagating S-wave.

Multicomponent seismic recording (measurement with vertical- and horizontal-component geophones and possibly a hydrophone or microphone) captures the seismic wavefield more completely than conventional single-element techniques.

In this paper, we describe the principle of converted waves and the resulting seismic processing procedures. Then, we explain the Kirchhoff prestack migration which is based on the equivalent offset migration (EOM). Then, we define EOM and the principle of P-S prestack migration by equivalent offset, and discuss the effect of using a single velocity V_c to create a gather with limited offset.

CONVERTED WAVES

Converted wave are usually data have a P-wave source, convert to S-wave at a reflector, and then recorded at the surface as a S-wave. These P-S surveys use conventional sources, but require several times more recording channels per receiving location and some special processing. The data quality of modern P-S sections approach

and in some cases exceeds the quality of conventional P-P seismic data (Steward et al, 2002).

P-S surveys were proposed and tried in the late 1970's and their processing fundamental in the 1980's to early 1990's. P-S surveys had not been implemented widely in hydrocarbon exploration in the past. Some reasons are: a) there were few multicomponent sensors available, b) challenging logistics in planting and cabling them, and c) the limitation in the recording equipment that requires three time the normal channels per station. Also, design and processing software were not commercially available and the data was difficult to interpret because few S-wave velocity logs had been acquired. All these limitations have now been overcome.

P-S design and processing software exists, geophones and recording channels are available, there are less logistical difficulties, S-wave logging is more commonly acquired, interpretative software is available and there are impressively successful case histories.

Converted waves have more applications than conventional P-wave, which includes structural imaging, lithologic estimation, anisotropy analysis, subsurface fluid description and reservoir monitoring. In addition, they are relatively inexpensive, broadly applicable, and an effective way to get S-wave information. (Steward et al., 2002).

Converted wave overview

The reflection/refraction/transmission of acoustic waves has been visualized as a simple geometry problem following Snell's law and a partitioning of energy between the reflected /transmitted energy across an interface between two media of contrasting acoustic properties. In an elastic medium, the problem is more complex, because it involves mode-conversion from P- to S wave, or S- to P-wave associated with both the reflection and refraction process.

Figure 1 shows the simplest elastic case of a P-wave striking a horizontal interface between two elastic solids. Four different waves are generated as result of the interaction of a single P-wave with the interface: a reflected P-wave, a reflected mode-converted SV-wave, a transmitted/refracted P-wave and a transmitted/refracted S-wave.

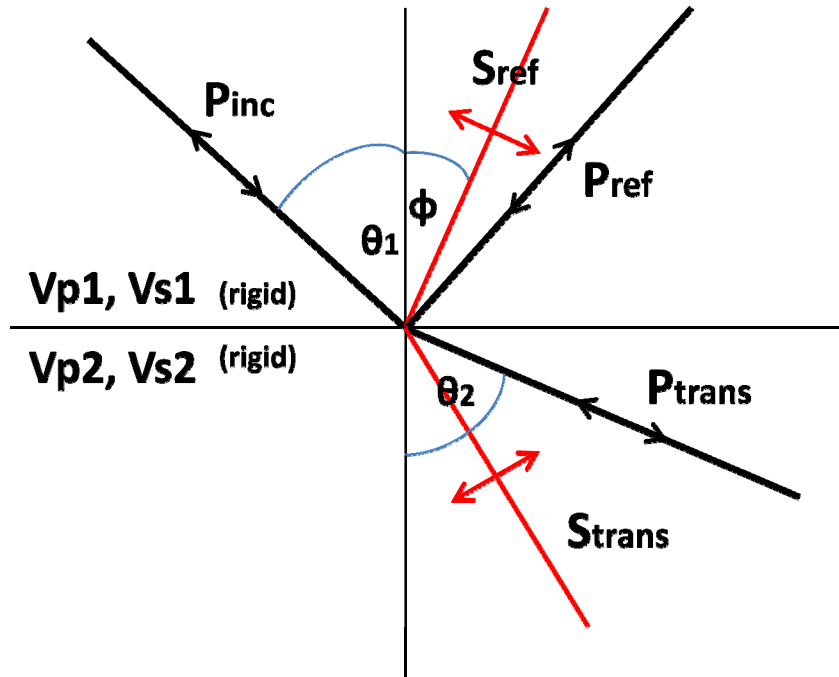


FIG. 1. Partitioning of energy into different waves types upon reflection and refraction. Reflected and refracted waves when a P-wave propagating in a solid and intersecting an interface to a different solid. Taken and modified from Tatham et al., 1998

In the case when the initial medium is liquid, there is no reflected/mode-converted S-wave, because liquid does not support S-wave propagation. Therefore, only three waves leave the interface: a reflected P-wave, a transmitted/refracted P-wave and a transmitted/refracted S-wave. This situation is common in marine acquisition. (Tatham et al., 1998)

Figure 1 shows an incident ray as a P-wave at θ_1 from the vertical and the reflected or mode-converted S-wave ray at an angle ϕ . The two angles are related by Shell's Law:

$$\frac{\sin \theta_1}{V_{p1}} = \frac{\sin \theta_2}{V_{p2}} = \frac{\sin \phi}{V_{s1}} = p, \quad (1)$$

where θ_1 is the P-wave angle of incidence, ϕ is the S-wave angles of reflection, θ_2 is the P-wave angle of refraction, V_{p1} and V_{s1} are the P- and S-wave velocities for the first medium, V_{p2} is the P-wave velocity for the second medium, and p is the ray parameter.

From Figure 2 it is possible to observe some characteristics of P-S converted wave reflections that make them different and of particular interest compared to P-P wave reflections traditionally used in seismic exploration. V_s is lower than V_p , ϕ is lower than θ , therefore, S-wave leaves the interface closer to perpendicular than P-wave does.

Due to different P and S velocities, the ray path geometry of the two types of reflections are different. When dealing with converted waves, the same reflection point for different sources and receivers is known as the common conversion point (CCP), since this is where the P energy is converted into shear energy. This reflection point is no longer at the common midpoint (CMP) between the source and receiver that we use in P-

P reflections. Furthermore, the CCP for P-S reflections is depth-dependent, even for horizontally layered media, such that, traditional processing techniques must be modified for this new geometry.

Converted wave processing consideration

Stacking is the sum data with the same reflection point. For P-P data, this point is midway between the source and the receivers. Stacking technique for common reflection data is usually used in reflection seismology to attenuate multiples and random noise, and to estimate the subsurface velocity distribution. The application of this technique to converted waves of P-S type is not as simple as for P-P or S-S reflections, which have symmetrical ray paths. The path for a converted wave is asymmetrical (as shown in Figure 3), even for a simple, horizontal layered medium, and the conversion point is not midway between sources and receivers. (Tessmer, et al., 1988)

Figure 3 shows some schematic raypaths, converting at various reflectors. The vertical dotted line at the left, is the midpoint, where all these rays reflect for P-P reflection. The dashed line at the right is the asymptotic approximation given by the conversion point at infinite depth.

Converted waves staking requires a common conversion point to be computed. The sorting of traces with a CCP depends on the depth of the reflector and the ratio V_p/V_s . For a single, horizontal, homogeneous layer, if the source-receiver offset is small relative to the depth of the conversion point, a first-order approximation for the location k of a CCP from the source point can be computed from a simplified relation:

$$k_{asympt} = \frac{2h}{1 + \left(\frac{V_s}{V_p}\right)}, \quad (2)$$

where $2h$ is the source-receiver offset (Tessmer et al., 1988). Binning base in equation (2) is called asymptotic CCP binning. This asymptotic CCP algorithm is simple and fast. It is only a first-order approximation of the true conversion point.

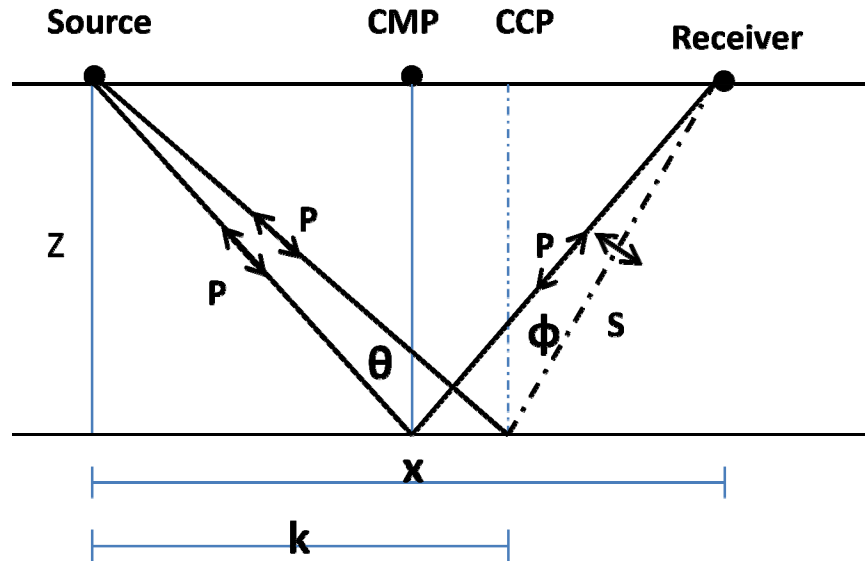


FIG. 2. A converted wave (P-S) reflection at its common conversion point (CCP) compared to a pure P-wave reflection at its common mid-point (CMP). Taken and modified from Stewart et al., 2002

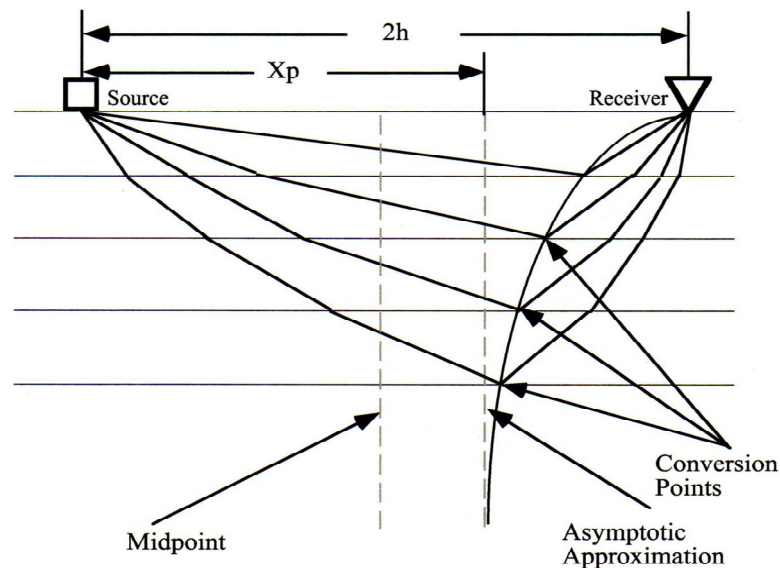


FIG. 3. Schematic diagram for 2-D common conversion point (CCP) binning. Taken from Wang, 1997

To obtain focusing for a single reflector at an arbitrary depth, the conversion point coordinate k must vary with depth. The conversion point of a single horizontal reflector can be calculated as a function of the reflector depth z and the velocity ratio V_p/V_s for a given offset h . Tessmer et al., 1988 explain depth-variant CCP method binning more accurate but this method is very time consuming.

The ratio of compressional and shear-wave velocity V_p/V_s , defined as γ , is:

$$\gamma = \frac{V_p}{V_s}. \quad (3)$$

Its value depends on physical assumptions, such as vertical homogeneity and/or isotropy.

Because the angles of incident and reflected vary considerably with depth, we can simplify the case for deep and shallow reflectors.

Case (1) Deep reflector:

When we consider a deep reflector, the angle of incident is very small, and we can approximate $\sin \theta \sim \theta$, as in Figure 4a. In this case, the equation (1) can be write as

$$\frac{\theta_i}{\theta_r} = \frac{V_p}{V_s} = \gamma. \quad (4)$$

From the geometry,

$$\tan \theta_i = \frac{k}{z}, \quad (5)$$

and

$$\tan \theta_r = \frac{(2h-k)}{z}. \quad (6)$$

Using the approximation for small angles, $\tan \theta \sim \sin \theta \sim \theta$, we get:

$$k = \frac{2h\gamma}{1+\gamma}, \quad (7)$$

for $\gamma=2$,

$$k = \frac{4}{3} h. \quad (8)$$

Case (2) Shallow reflector:

For the shallow case, we can assume θ_i to be almost 90° , then from the equation (1) we can get:

$$\frac{1}{\sin \theta_r} = \gamma, \quad (9)$$

or $\sin \theta_r = 1/\gamma$.

From the geometry,

$$\tan \theta_r = \frac{2h-k}{z}, \quad (10)$$

or

$$k = 2h - z \tan \theta_r, \tag{11}$$

For $\gamma=2$, $\sin \theta_r \sim 1/2$. Therefore, $\theta_r = 30^\circ$ and

$$k \sim 2h. \tag{12}$$

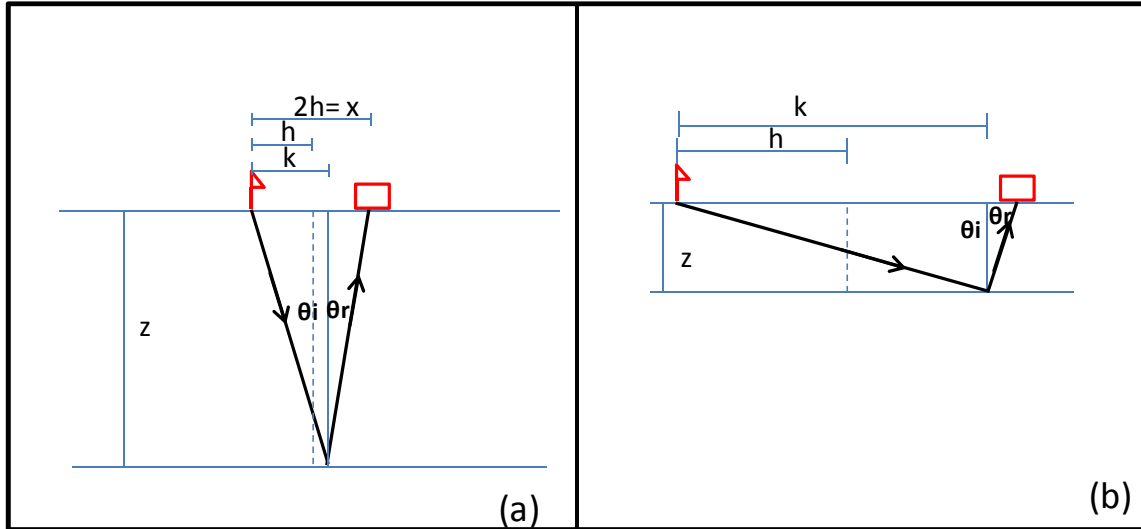


FIG. 4 Case (a) for deep reflector. (b) for shallow reflector

From equations (8) and (12) we get the solution for k , the distance for converted common point from the source. This distance varies according with the depth of the interface.

Kirchhoff Prestack Migration concepts

The purpose of migration is to construct an image of the subsurface from seismic reflection data. Prestack migration is a direct process that moves each input sample into all the possible reflection positions, and invokes the principles of constructive and destructive interference to recreate the actual image. All traces are searched to find energy that contributes to the output sample.

Kirchhoff prestack migration is based on a model of the subsurface as an organized set of scattered points. The model assumes that energy may come from a source located anywhere on the surface to all receivers. The location of energy on a recorded trace is the total travel time along the ray path from the source down to the scatter point and back up to the receiver. Kirchhoff prestack migration assumes an output location, and then sums the appropriate energy from all available input traces.

The surface position of a vertical array of scatter points is referred to as the common scatter point (CSP) location. The collection of all input traces that record energy from a given scatter point is referred as the migration aperture.

From the raypaths showed in Figure 5, the traveltime t is estimated by the adding the time from the source to the scatter point t_s and time from the scatter point to the receiver t_r , or

$$t = t_s + t_r. \tag{13}$$

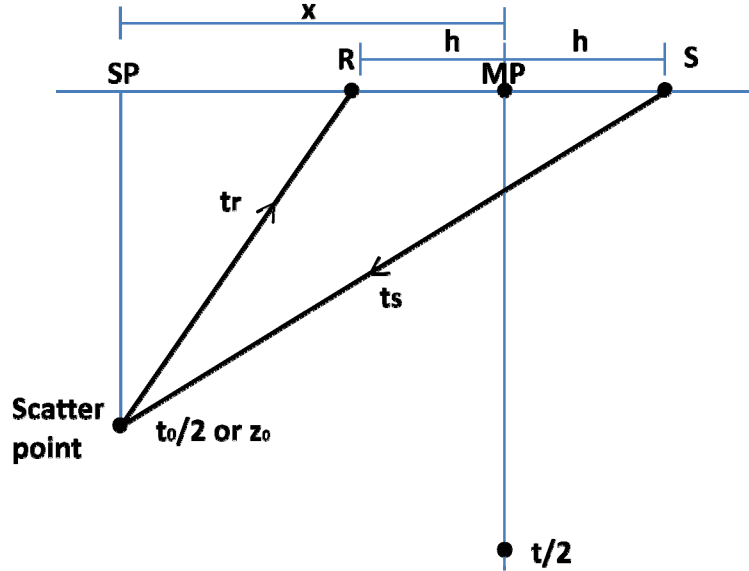


FIG. 5. Geometry for Kirchhoff prestack time migration with source S and receiver R. The total travel time is the sum of source to scatterpoint time t_s and the scatterpoint to receiver time t_r . Taken from Bancroft et al. 1998.

From the geometry, the total or two-way, travel time can be computed from:

$$t = \left[\left(\frac{t_0}{2} \right)^2 + \frac{(x+h)^2}{V_{mig}^2} \right]^{1/2} + \left[\left(\frac{t_0}{2} \right)^2 + \frac{(x-h)^2}{V_{mig}^2} \right]^{1/2}, \tag{14}$$

where x is the location of the source-receiver midpoint (MP) relative to the scatter point (SP) located at $x=0$, and V_{mig} is the RMS migration velocity evaluated at t_0 . The time $t_0=t(x=0, h=0)$ is the two-way zero-offset time and t_0 is defined from the data. We can defined

$$z_0 = \frac{t_0 V_{ave}}{2}. \tag{15}$$

The equation (14) is known as the double square root (DSR) equation and defines the traveltimes surface over which the Kirchhoff summation or integration takes places.

EQUIVALENT OFFSET MIGRATION

The equivalent offset is defined by converting the DSR equation (14) into an equivalent single square root or hyperbolic form (Bancroft et al., 1998). This can be reformulated by defining a new source and receiver collocated at the equivalent offset position E as illustrates Figure 6. For convenience, the CSP gather is located at $x=0$. The equivalent offset h_e is chosen to maintain the same traveltime from equation (13):

$$t = 2t_e = t_s + t_r. \tag{16}$$

This travel times can be written as:

$$2 \left[\left(\frac{t_0}{2} \right)^2 + \frac{h_e^2}{v_{mig}^2} \right]^{1/2} = \left[\left(\frac{t_0}{2} \right)^2 + \frac{(x+h)^2}{v_{mig}^2} \right]^{1/2} + \left[\left(\frac{t_0}{2} \right)^2 + \frac{(x-h)^2}{v_{mig}^2} \right]^{1/2}. \tag{17}$$

This equation may be solved for the equivalent offset h_e to get:

$$h_e^2 = x^2 + h^2 - \left(\frac{2xh}{tV_{mig}} \right)^2. \tag{18}$$

The equivalent offset is a quadratic sum of the distance x between the CSP and the CMP, and h , the source-receiver half offset.

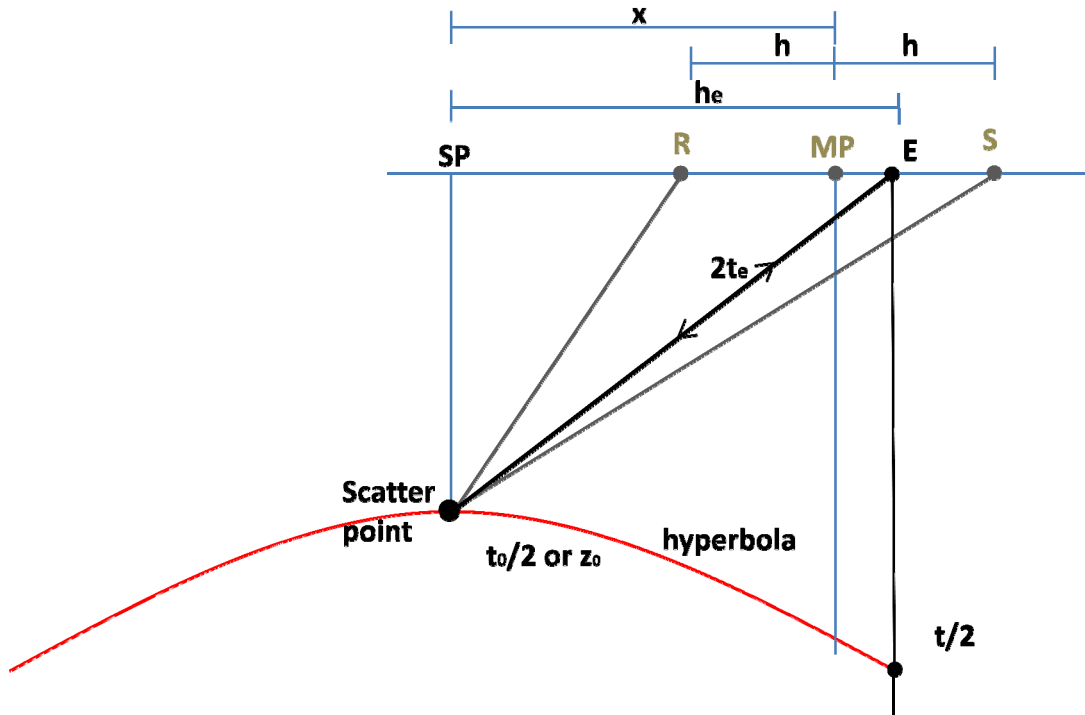


FIG. 6. Equivalent offset h_e is defined as the offset from the surface to a collocated source-receiver having h_e same traveltime as the original source-receiver. Scattered energy from all source pairs lies along the hyperbola at their equivalent offset. Taken from Bancroft et al., 1998.

Equivalent offset migration forms prestack migration gathers, called scatter points (CSP) gathers. Reflection energy in the gathers is hyperbolic with RMS type velocity. (Bancroft, 1995)

After the CSP gathers have been formed, the filtering, scaling, and time shifting, collapse the energy on the CSP gather to zero offset to form a prestack migrated trace.

The gathers have high fold and offsets that can be greater than the maximum source-receiver offset. This high fold improves the resolution of velocity analysis over conventional CMP gathers. After velocity analysis, NMO and stacking completes the prestack migration. EOM result will be the same result as prestack Kirchhoff time migration, but with shorter run times. The method is easy to implement, and uses the current processing algorithm such as velocity analysis. (Bancroft, 1995)

Converted wave migration using EO concept

Converted wave processing assumes the downward propagating energy is a P wave and reflection energy a shear wave. This S-wave is recorded with 3 component receivers; proving additional information of the subsurface. The processing methods start with the DSR equation (14) or (17), with the appropriate P and S velocities for each leg of the ray path, as illustrate in Figure 7.

From equation (13) and using the concepts of prestack time migration and RMS velocities for both, the P-wave and S-wave energy, the travel time is defined by:

$$t = \left[\left(\frac{t_{0p}}{2} \right)^2 + \frac{h_s^2}{V_{p-rms}^2} \right]^{1/2} + \left[\left(\frac{t_{0s}}{2} \right)^2 + \frac{h_r^2}{V_{s-rms}^2} \right]^{1/2}, \quad (19)$$

where V_{p-rms} and V_{s-rms} are the respective RMS velocities for P and S waves. The vertical zero offset time are t_{0p} and t_{0s} . The distances h_s , and h_r are shown in Figure 7. We now replace t_{0p} and t_{0s} by z_0 , stating with the average velocities

$$z_0 = \frac{t_{0p} V_{p-ave}}{2} = \frac{t_{0s} V_{s-ave}}{2}. \quad (20)$$

Replacing t_0 by z_0 , we get:

$$t = \left[\left(\frac{z_0}{V_{p-ave}} \right)^2 + \frac{h_s^2}{V_{p-rms}^2} \right]^{1/2} + \left[\left(\frac{z_0}{V_{s-ave}} \right)^2 + \frac{h_r^2}{V_{s-rms}^2} \right]^{1/2}. \quad (21)$$

$$t = \frac{1}{V_{p-rms}} \left[\left(\frac{z_0 V_{p-rms}}{V_{p-ave}} \right)^2 + h_s^2 \right]^{1/2} + \frac{1}{V_{s-rms}} \left[\left(\frac{z_0 V_{s-rms}}{V_{s-ave}} \right)^2 + h_r^2 \right]^{1/2}. \quad (22)$$

The same travel-time t for the equivalent offset h_e is given by:

$$t = \frac{1}{V_{p-rms}} \left[\left(\frac{z_0 V_{p-rms}}{V_{p-ave}} \right)^2 + h_e^2 \right]^{1/2} + \frac{1}{V_{s-rms}} \left[\left(\frac{z_0 V_{s-rms}}{V_{s-ave}} \right)^2 + h_e^2 \right]^{1/2}. \quad (23)$$

We now assume

$$\frac{V_{p-rms}}{V_{p-ave}} \approx \frac{V_{s-rms}}{V_{s-ave}} \approx \frac{V_{rms}}{V_{ave}}, \quad (24)$$

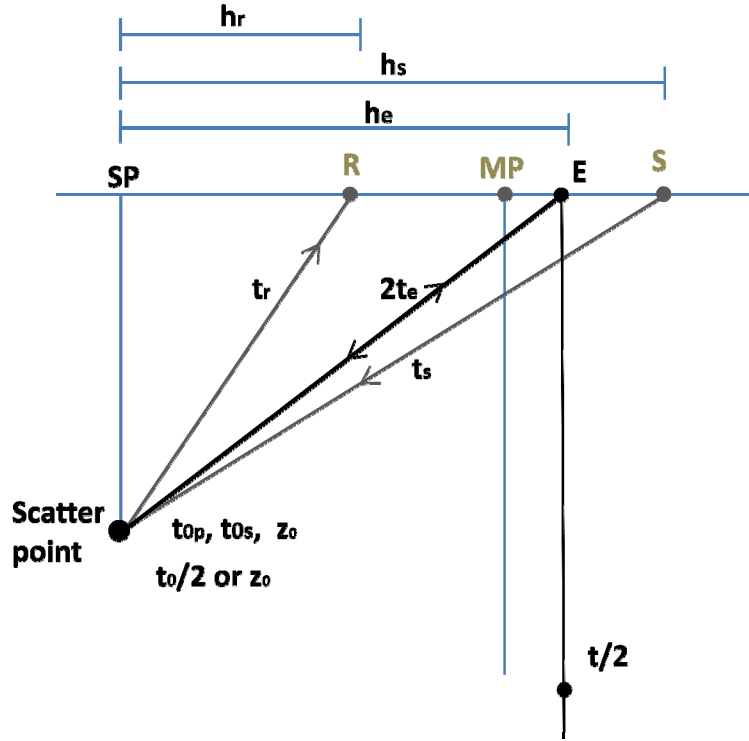


FIG. 7. The raypaths and travel time for a scatter or conversion point.

then

$$\hat{z}_0 = z_0 \frac{V_{rms}}{V_{ave}}. \quad (25)$$

We can rewrite equation (23) as

$$t = \frac{1}{V_{p-rms}} \sqrt{\hat{z}_0^2 + h_e^2} + \frac{1}{V_{s-rms}} \sqrt{\hat{z}_0^2 + h_e^2}, \quad (26)$$

or

$$t = \left(\frac{1}{V_{p-rms}} + \frac{1}{V_{s-rms}} \right) \sqrt{\hat{z}_0^2 + h_e^2}. \quad (27)$$

This equation can also be written as

$$t = \frac{2}{V_{c-rms}} (z_0^2 + h_e^2)^{1/2}, \quad (28)$$

where V_{c-rms} is defines as

$$V_{c-rms} = \frac{2V_{p-rms}V_{s-rms}}{V_{p-rms} + V_{s-rms}} = \frac{2V_{p-rms}}{(1+\gamma)}. \quad (29)$$

The equivalent offset h_e can then be defined as:

$$h_e^2 = \frac{t^2 v_c^2}{2} - \hat{z}_0^2. \quad (30)$$

From the equation (30), the equivalent offset h_e is a function of travel time t , and is also velocity and depth-dependent.

An equivalent offset method of migrating converted wave migration has been developed and works successfully. During this process we estimate a converted wave velocity V_c from the hyperbolic moveout on a CSP gather. Moveout (MO) correction and stacking completes the prestack migration. We obtain V_c from equating the zero offset traveltimes with the original offset traveltimes.

$$\frac{1}{v_p} \sqrt{\hat{z}_0^2 + h_s^2} + \frac{1}{v_s} \sqrt{\hat{z}_0^2 + h_r^2} = \left(\frac{1}{v_p} + \frac{1}{v_s} \right) \sqrt{\hat{z}_0^2 + h_e^2} = \frac{2}{v_c} \sqrt{\hat{z}_0^2 + h_e^2}, \quad (31)$$

where, h_e can also be redefined as

$$h_e^2 = \frac{v_c^2}{4} \left(\frac{1}{v_p} \sqrt{\hat{z}_0^2 + h_s^2} + \frac{1}{v_s} \sqrt{\hat{z}_0^2 + h_r^2} \right)^2 - \hat{z}_0^2. \quad (32)$$

Extending the use of the converted wave velocity V_c

The velocity V_c is used to apply moveout correction on the converted wave CSP gathers. Is it possible to ignore V_p and V_s and simply use V_c as a velocity for the entire input data. We know that

$$t_{p-s} = \frac{1}{v_p} \sqrt{z_0^2 + h_s^2} + \frac{1}{v_s} \sqrt{z_0^2 + h_r^2}, \quad (33)$$

and now we define time t_{V_c} assuming constant velocity of the media V_c ,

$$t_{V_c} = \frac{1}{v_c} \sqrt{z_0^2 + h_s^2} + \frac{1}{v_c} \sqrt{z_0^2 + h_r^2}. \quad (34)$$

How close is t_{V_c} to t_{ps} ? Given $h_s = x + h$ and $h_r = x - h$, and if we assume either $x=0$ or $h=0$, then $t_{h \text{ or } x=0} = t_{V_c}$. For all other conditions,

$$t_{h \text{ or } x \neq 0} \neq t_{V_c}. \quad (35)$$

However, can we tolerate a small error in t_{V_c} , say 5 ms or 10 ms that will allow us to collect near offset traces into a gather for velocity analysis. Note, the reflected energy of the converted wave is zero when the offset is zero. If so, we may get enough traces into a limited converted wave CSP (LCCSP) gather to quickly and accurately estimate V_c . If this is possible, our goal is to identify the range of h , Δh , given an x value, and the range of x , Δx given an h value for an acceptable LCCSP gather.

Figure 8 was created to illustrate the error z that can be expected for offset ranges h , and depth z . This figure also illustrated the error as a function of depth and offset.

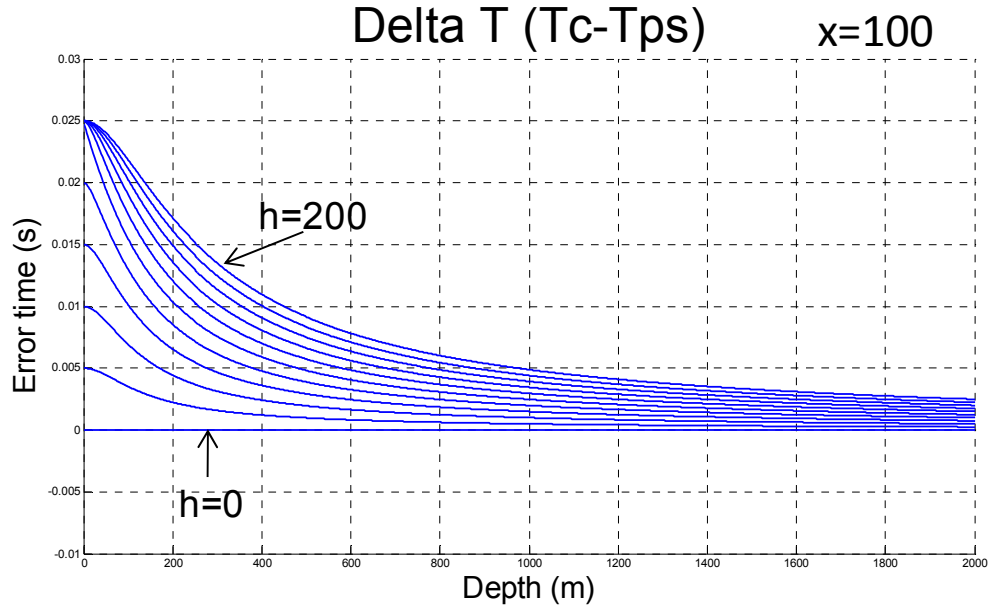


FIG. 8. Error time for different source-receiver half offset h (from 0 to 200 m), in increment of 20 m for constant velocities. $V_p=4000$ m/s, $V_s=2000$ m/s, distance between the CSP and CMP $x=100$ m.

From the equation (32), h_e varies with the trace geometry h_s , and h_r , but also varies with depth \widehat{z}_0^2 and the velocity $V_c(z_0)$, as V_p can also be a function of depth \widehat{z}_0^2 .

We now ask what are the limits on h_e for the two cases as the depth tends to zero or to infinity.

The asymptotes of h_e at the first usable sample is $h_{e\alpha}$. At large time, t tends to $h_{e\omega}$.

We want to know the limiting behaviors of the curves at both limits ($z_0 \rightarrow 0$ and $z_0 \rightarrow \infty$) from equation (31), they are:

Case $z_0 \rightarrow 0$:

Substituting (29) in (32) h_e can be defined as:

$$h_{e\alpha} = \frac{(h_s + \gamma h_r)}{1 + \gamma}, \tag{36}$$

details are shown in Appendix A.

Case $z_0 \rightarrow \infty$:

Substituting (29) in (32):

$$h_{e\omega}^2 = \frac{1}{(1+\gamma)^2} \left(\sqrt{z_0^2 + h_s^2} + \gamma \sqrt{z_0^2 + h_r^2} \right)^2 - z_0^2. \quad (37)$$

The expression $(1+x)^{1/2}$ can be written as

$$(1+x)^{1/2} = 1 + \frac{x}{2} - \frac{x^2}{8} + \frac{x^3}{16} + \dots \quad (38)$$

When x is very small,

$$(1+x)^{1/2} \approx \left(1 + \frac{x}{2}\right). \quad (39)$$

Substituting (39) in (37) allows h_e to be defined as:

$$h_e^2 = \frac{(h_s^2 + \gamma h_r^2)}{1+\gamma}, \quad (40)$$

details of definitions are shown in Appendix 2.

These two asymptotes function define the range of offsets from the samples in the input trace.

Using the values, $V_p=4000$ m/s, $V_s=2000$ m/s, the distance between the CSP and CMP $x=100$ m, and source-receiver half offset $h=50$ m, the equivalent offset h_e is between 83.33 m (case $z_0 \rightarrow 0$) and 95.74 m (case $z_0 \rightarrow \infty$). Figure 9 shows a CSP gather with one trace, with values specified above.

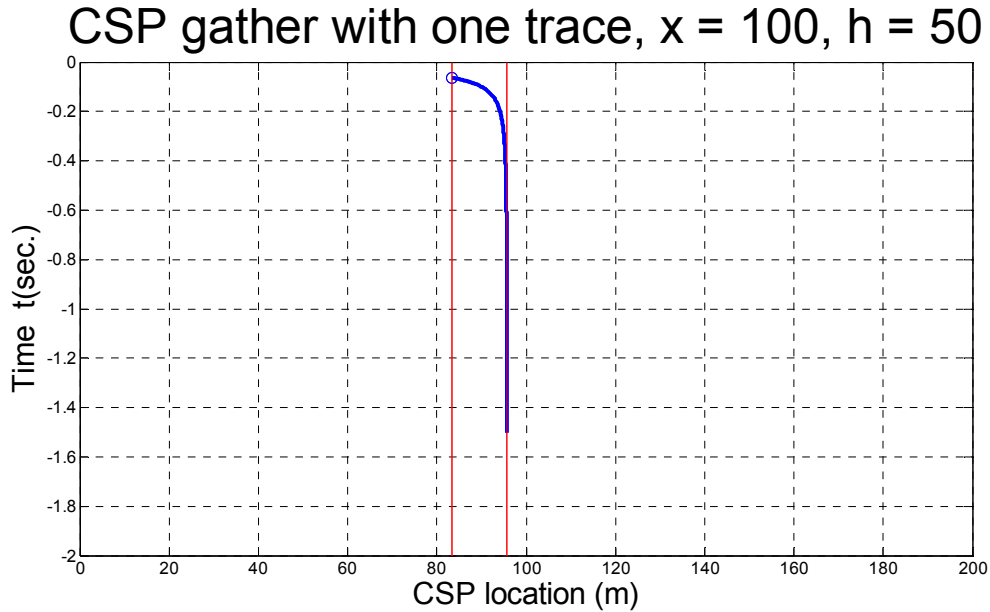


FIG. 9. Equivalent offset for constant velocity $V_p=4000$ m/s, $V_s=2000$ m/s, $x=100$ m, $h=50$ m

The Figure 10 shows h_e curves at different CSP surface locations, calculated using the equation (30). Using the values, $V_p=4000$ m/s, $V_s=2000$ m/s, the distance between the CSP and the CMP $x=$ from 200 to 2000 m with increment of 200 meters, and source-

receiver half offset $h=200$ meters. Note how the equivalent offset tends to the asymptotic values as t increases. Also, how h_e starts at different t with increment of x .

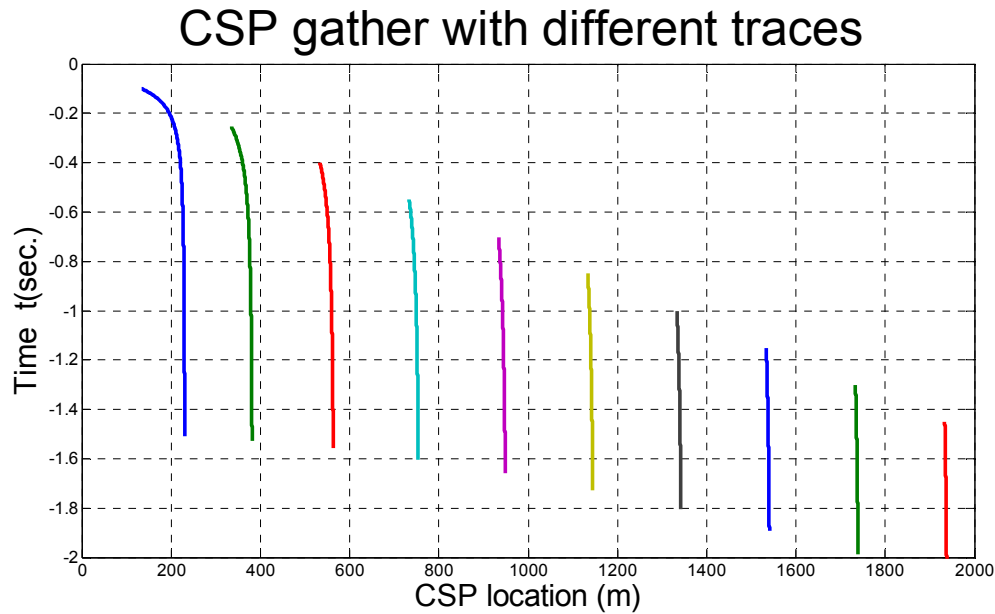


FIG. 10. Equivalent offset for constant velocity $V_p=4000$ m/s, $V_s=2000$ m/s, $x=200-2000$ m, $h=200$ m.

We now assume a vertical array of scatterpoints at depth z from 0 to 1000 m that are at a spatial location of $x = 0$. A range of mid-point locations are located to the left and right of this vertical array, with distance x , i.e. $x = -1000$ to 1000 m. We then assume a fixed value for a half-offset h_{con} . Two-way traveltimes were then computed to and from the scatterpoint as a function of x and z , i.e., $t(x, z, h = h_{con})$. This was repeated for t_{Vc} and the plots are shown in Figure 11, where h_{con} was chosen to be 50 m.

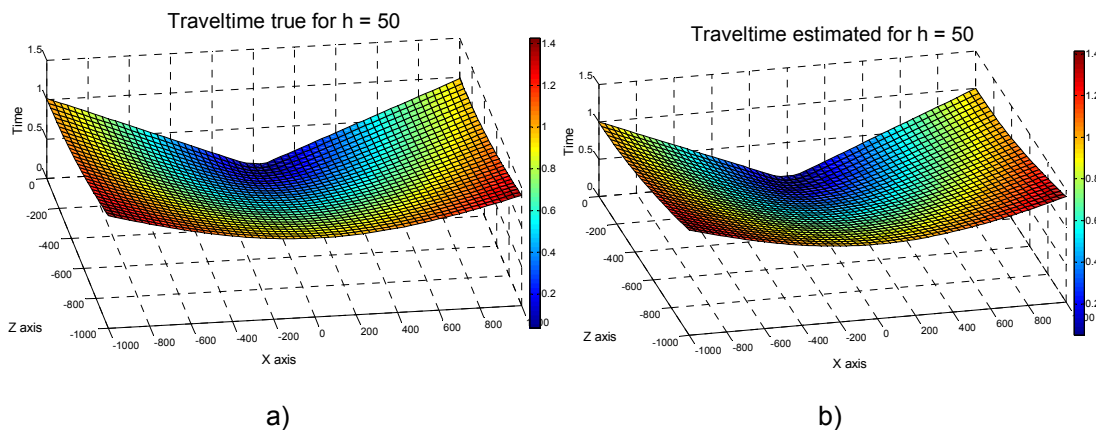


FIG. 11. Travel time for one vertical array of scatterpoints at $x = 0$, with a) the true traveltimes and b) the traveltimes computed assuming a constant converted wave velocity for $h = 50$ m.

With a half-offset of 50 m, the difference in the two traveltimes is difficult to view, so the following plot shows the difference in traveltimes, and the magnitude of the difference in traveltimes.

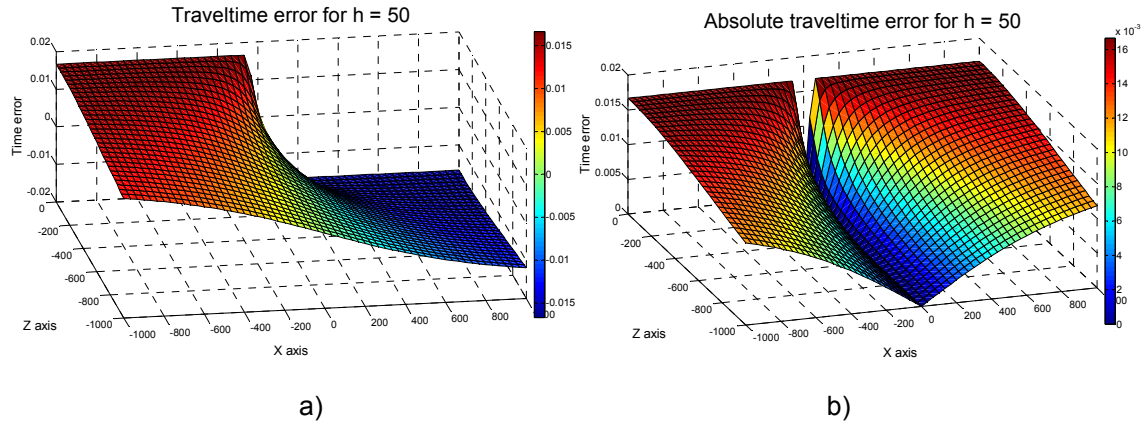


FIG. 12. Travel time differences with a) the actual time and b) the magnitude value of the traveltime.

We can see in Figure 12a that the traveltime error ranges from -15 ms to approximately +15 ms. If we limit the absolute traveltime difference in Figure 12b to a maximum of 10 ms, then the data in traces that have geometry in the blue hue could be used. Figure 12a illustrates there is an opposite polarity of the time error. Stacking traces with an opposing time differences will lower the frequency content of these traces, but will not introduce a time shift bias in the data. Consequently, a larger time difference, say 20 ms, may be usable.

The absolute traveltime is plotted below in a plan view with the colour defining the absolute time difference, in Figure 13. The dimensions of this plot are in space and depth (x, z) representing the location of the midpoint and the depth of the scatterpoint for a fixed source-receiver offset h_{con} . These coordinates are not convenient for evaluating a LCCSP gather. We remap the data first to two-way time to and scatterpoint in time in Figure 14, and then to time and equivalent offset in Figure 15. Figure 15 now represents the location of energy on a CPS gather and we can see where the limited offset data will lie.

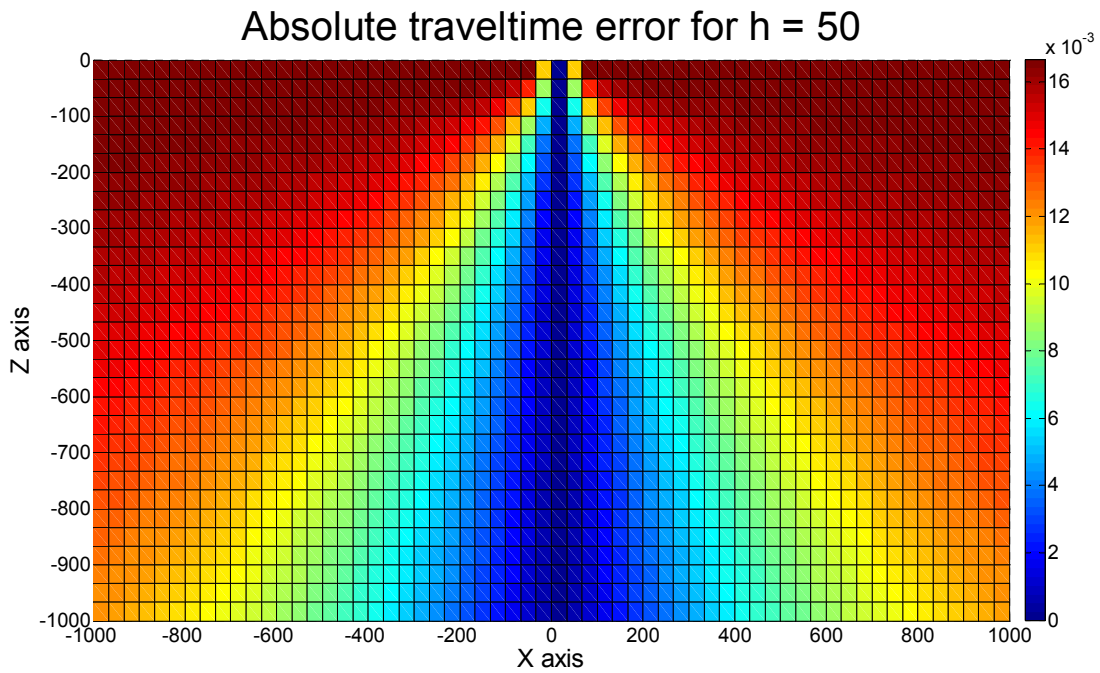


FIG. 13. Plan (or map view) of the absolute value of the traveltime difference.

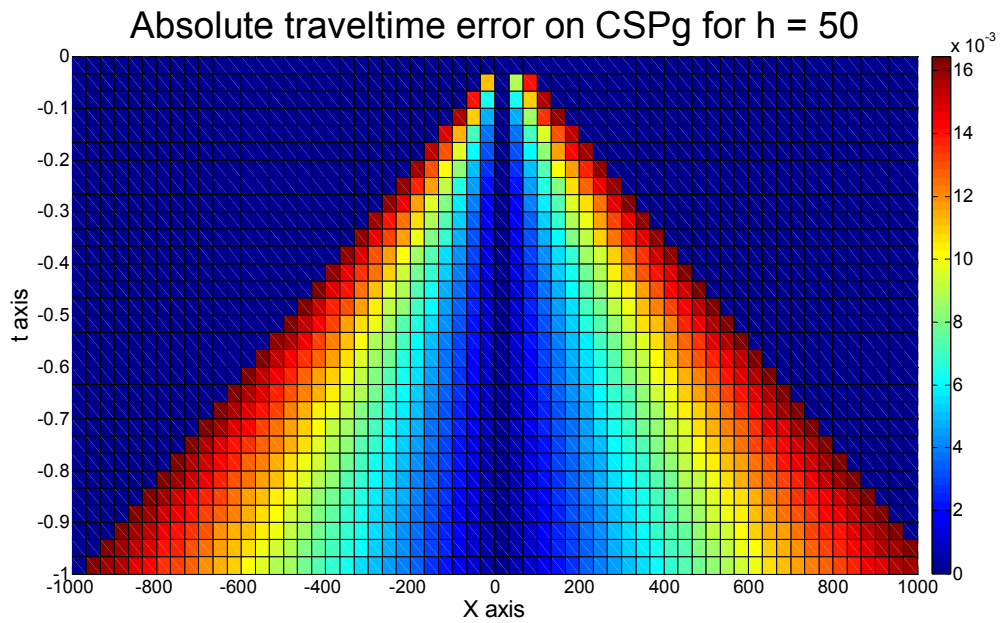


FIG 14. Traveltime error plotted as two-way time and depth.

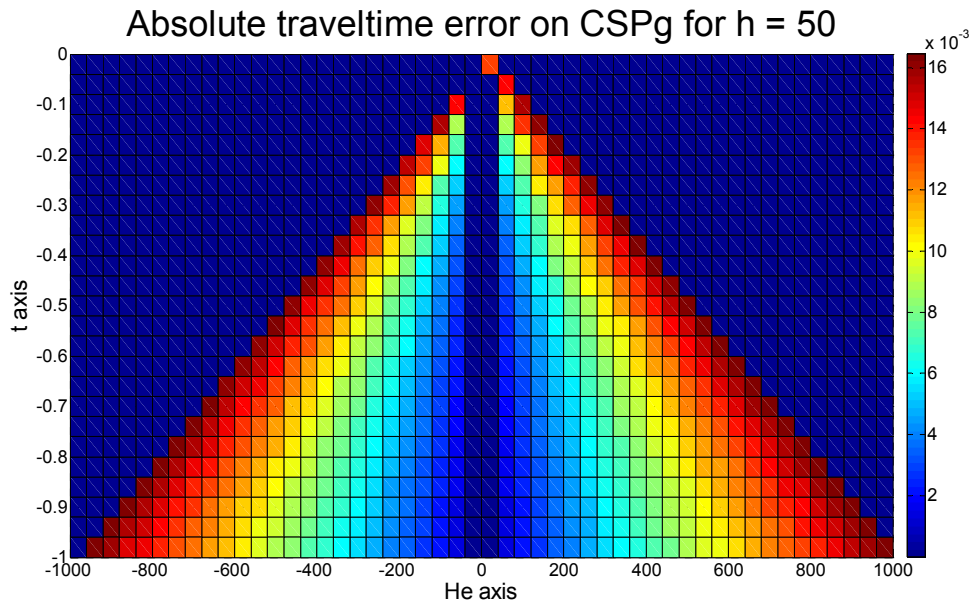


FIG. 15. Traveltime error plotted as two-way time and equivalent offset.

The following Figure 16 shows the travel time errors on CSP gathers views of various offsets of $h = 50, 100, 200,$ and 500 .

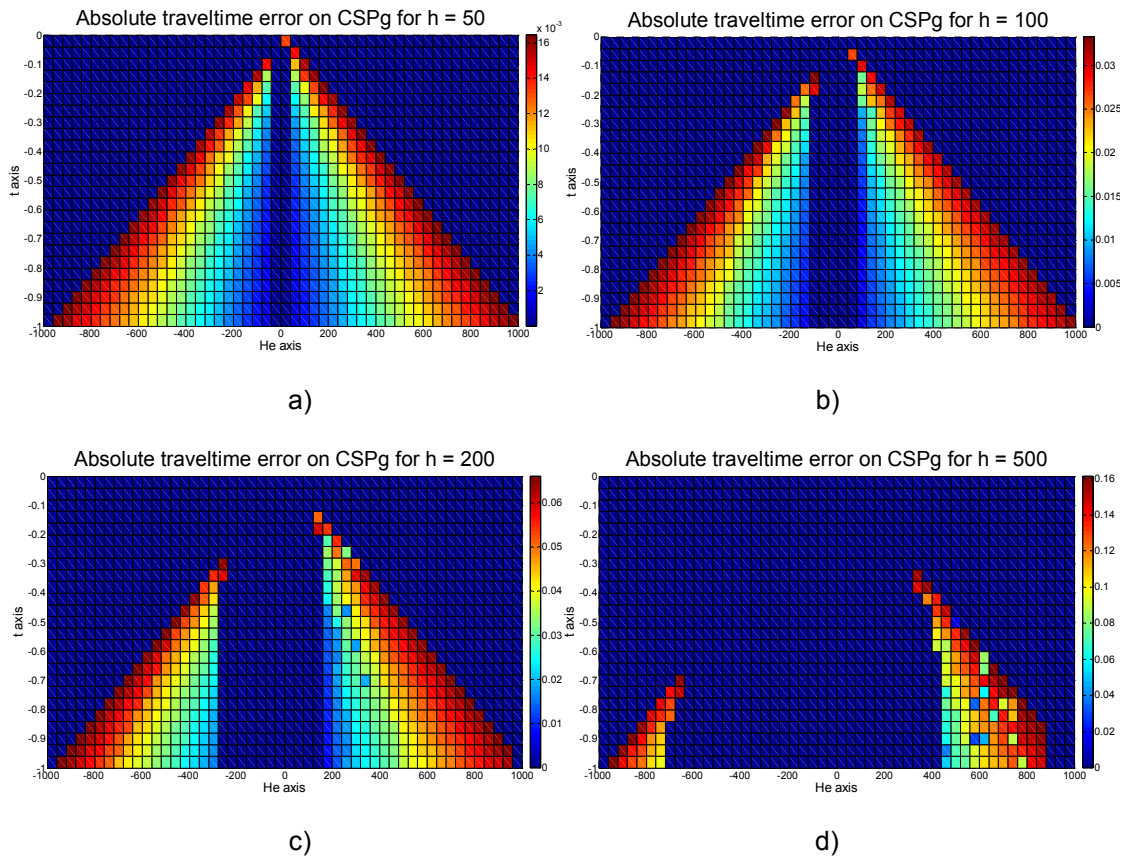


FIG. 16. Traveltime difference on a CSP gather for various half offsets h equal to: a) 50 m, b) 100 m, c) 2000 m, and d) 500 m. Note that the values on the time scale vary for each figure.

The previous figures assume the source is on the left and the receiver is on the right. The converted wave ray-paths are asymmetrical and produces an image that is asymmetrical about $x = 0$. Swapping the source-receiver locations will reverse the equivalent offsets. A center spread acquisition system will produce LCCSP gathers with opposite polarities of the traveltime difference that will tend to sum to zero and remove any bias in the gather.

A limiting value for the time difference could be equal to half the size of the positive part of the wavelet peak. Equal half shifts in the opposite direction may tend to cancel the wavelets.

Useable convert time

Converted wave CSP gather are formed by summing all input traces (within the migration aperture) at the equivalent offset. We now form a limited converted wave CSP (LCCSP) gather assuming a single velocity V_c define in equation (29). This equation is only valid for zero offset data, however we desire to extend its application when there is an acceptable error τ in the estimated traveltime.

Assume that we are given the geometry of a trace, x , and h , relative to the location of a given LCCSP gather. With an acceptable τ , we want to find the start time t_s , at which we will start to copy the remainder of the trace into the gather.

From equation (31), we derive the depth of a scatterpoint z_f that correspond to the time error τ .

$$z_f = \left[\frac{(h_s^2 + h_r^2 - k_1^2)^2 - 4 h_s^2 h_r^2}{4k_1^2} \right]^{1/2}, \quad (41)$$

where k_1 is defined as

$$k_1 = \frac{2V_p \tau}{1 - \gamma}, \quad (42)$$

details are shown in Appendix C.

From the depth z_f , we can then compute the true traveltime of t_f using equation (31), then the equivalent offset using

$$h_{ef} = \left(\frac{V_c^2 t_f^2}{4} - z_f^2 \right)^{1/2}. \quad (43)$$

The trace can then be summed into the LCCSP gather, starting at time t_f with equivalent offset h_{ef} . These traces do have a limited offset, and the range of the equivalent offsets in the following samples may be assumed to be the same of h_{ef} . This remains to be evaluated.

The following Figure (17) contains traveltime differences that were created for $h = 100$ and at a higher resolution. In addition, the first useable times t_f were computed as

above and plotted as “+” signs for a limiting time of $\tau = 20$ ms. Note the correspondence with the colour contour for 0.02 s.

The useable data in the traces appears to be quite large for a $\tau = 20$ ms. However, even for a smaller time difference, there may still be considerable trace energy to form a reasonable LCCSP gather.

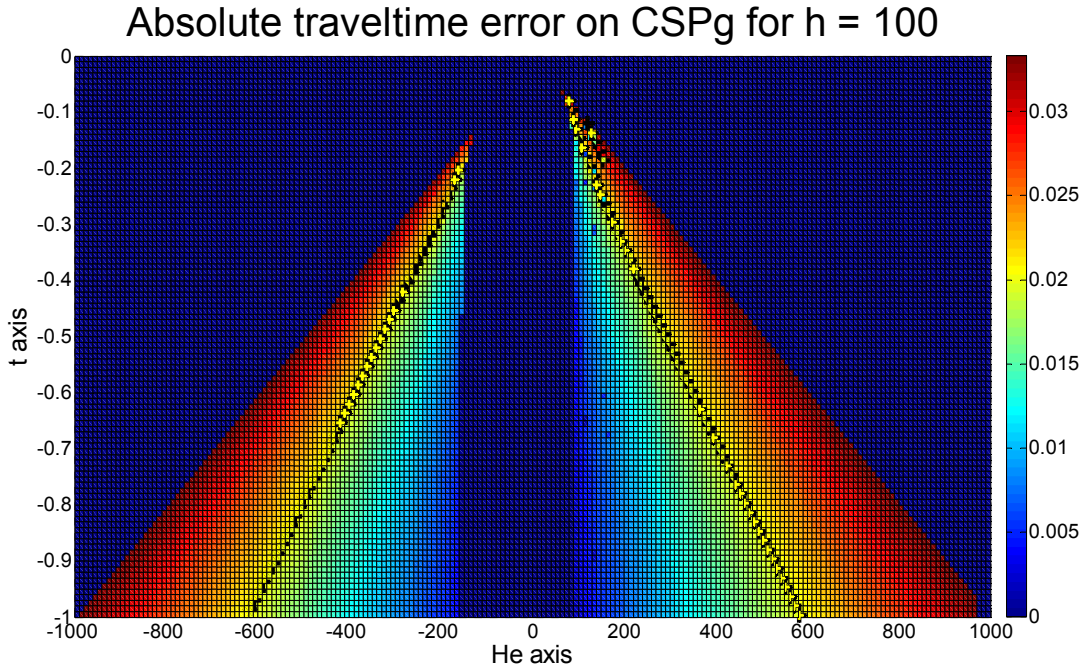


FIG. 17 Traveltme difference on a CSP gather for various half offsets for h equal 100 m, overlain with symbols computed for $\tau = 20$ ms.

CONCLUSION

Converted wave prestack migration by equivalent offset is based on the principles of Kirchhoff migration and uses equivalent offset to form limited converted CSP (LCCSP) gathers.

The DSR equation for prestack migration can be reformulated with an appropriate P and S velocities for each leg of the ray path. Using relation between these two velocities, a converted wave velocity can be estimated from the hyperbolic moveout on the CSP gathers.

An acceptable time error may be defined to form a LCCSP gather by assuming a constant converted wave velocity. The intended application is to rapidly form a LCCSP gather to provide an initial velocity model for converted wave prestack migration using the equivalent offset method.

The range of acceptable data is dependent on the P-wave velocity and an assumed S-wave velocity. However, the gather formed is independent of those velocities, and a more accurate S-wave velocity (or γ) is estimated.

ACKNOWLEDGMENTS

We thank to the sponsors of the CREWES Project for their support.

REFERENCES

- Bancroft, J.C., Geiger, H.D., and Margrave, G.F., 1998, The equivalent offset method of prestack time migration: *Geophysics*, **63**, 2042-2053
- Bancroft, J., Geiger, H., and Foltinek, D., 1994, Prestack migration by equivalent offset and CSP gathers: CREWES Research Report, 6, 27.1-27.13.
- Bancroft, J., Geiger, H., Wang, S., and Foltinek, D., 1995, Prestack migration by equivalent offset and CSP gathers: an update: CREWES Research Report, 7, 27.1-27.
- Bancroft, J., Wang, S., 1994, Converted-wave prestack migration and velocity analysis by equivalent offsets and CCP gathers: CREWES Research Report, 6, 28.1-28.7
- Stewart, R.R., Gaiser, J.E., Brown R.J., and Lawton, D.C., 2002, Tutorial: Converted-wave seismic exploration: *Methods, Geophysics*, **67**, 1348-1363.
- Tatham R., and McCormack, M., 1998, Multicomponent seismology in Petroleum Exploration: SEG publications
- Tessmer, G., and Behle, A., 1988, Common reflection point data-staking technique for converted waves: *Geophysics Prospecting*, **36**, 671-688
- Wang, S., 1997, Three-component and three-dimensional seismic imaging,

APPENDIX A

Starting with the definition for the equivalent offset equation (32), we have

$$h_e^2 = \frac{V_c^2}{4} \left(\frac{1}{V_p} \sqrt{\hat{z}_0^2 + h_s^2} + \frac{1}{V_s} \sqrt{\hat{z}_0^2 + h_r^2} \right)^2 - \hat{z}_0^2. \quad (\text{A-1})$$

When $z_0 \rightarrow 0$

$$h_{e_{z_0 \rightarrow 0}}^2 = \frac{V_c^2}{4} \left(\frac{h_s}{V_p} + \frac{h_r}{V_s} \right)^2, \quad (\text{A-2})$$

if V_c is defines as

$$V_c = \frac{2V_p}{1+\gamma}, \quad (\text{A-3})$$

and V_s is defined as

$$V_s = \frac{V_p}{\gamma}, \quad (\text{A-4})$$

then

$$h_{e_{z_0 \rightarrow 0}}^2 = \frac{V_p^2}{(1+\gamma)^2} \left(\frac{h_s}{V_p} + \frac{\gamma h_r}{V_s} \right)^2, \quad (\text{A-5})$$

therefore

$$h_{e_{z_0 \rightarrow 0}}^2 = \frac{1}{(1+\gamma)^2} (h_s + \gamma h_r)^2, \quad (\text{A-6})$$

and finally

$$h_{e_{z_0 \rightarrow 0}} = \frac{(h_s + \gamma h_r)}{1+\gamma}. \quad (\text{A-7})$$

APPENDIX B

Starting with the definition for the equivalent offset equation (33), we have

$$h_e^2 = \frac{V_c^2}{4} \left(\frac{1}{V_p} \sqrt{\hat{z}_0^2 + h_s^2} + \frac{1}{V_s} \sqrt{\hat{z}_0^2 + h_r^2} \right)^2 - \hat{z}_0^2. \quad (\text{B-1})$$

When $z_0 \rightarrow \infty$

$$h_{e_{z_0 \rightarrow \infty}}^2 = \frac{4V_p^2}{4(1+\gamma)^2} \left(\frac{1}{V_p} (z_0^2 + h_s^2)^{1/2} + \frac{\gamma}{V_p} (z_0^2 + h_r^2)^{1/2} \right)^2 - z_0^2, \quad (\text{B-2})$$

$$h_{e_{z_0 \rightarrow \infty}}^2 = \frac{1}{(1+\gamma)^2} \left((z_0^2 + h_s^2)^{1/2} + \gamma (z_0^2 + h_r^2)^{1/2} \right)^2 - z_0^2. \quad (\text{B-3})$$

The expression $(1+x)^{1/2}$ can be written in this way:

$$(1+x)^{1/2} = 1 + \frac{x}{2} - \frac{x^2}{8} + \frac{x^3}{16} + \dots \quad (\text{B-4})$$

when x is very small,

$$(1+x)^{1/2} \approx \left(1 + \frac{x}{2}\right), \quad (\text{B-5})$$

therefore

$$h_{e_{z_0 \rightarrow \infty}}^2 = \frac{1}{(1+\gamma)^2} \left(z_0 \left(1 + \frac{h_s^2}{z_0^2}\right)^{1/2} + \gamma z_0 \left(1 + \frac{h_r^2}{z_0^2}\right)^{1/2} \right)^2 - z_0^2, \quad (\text{B-6})$$

$$h_{e_{z_0 \rightarrow \infty}}^2 = \frac{1}{(1+\gamma)^2} \left(z_0 \left(1 + \frac{h_s^2}{2z_0^2}\right) + \gamma z_0 \left(1 + \frac{h_r^2}{2z_0^2}\right) \right)^2 - z_0^2, \quad (\text{B-7})$$

$$h_{e_{z_0 \rightarrow \infty}}^2 = \frac{1}{(1+\gamma)^2} \left(z_0(1+\gamma) + \left(\frac{h_s^2}{2z_0} + \frac{\gamma h_r^2}{2z_0}\right) \right)^2 - z_0^2, \quad (\text{B-8})$$

$$h_{e_{z_0 \rightarrow \infty}}^2 = \frac{1}{(1+\gamma)^2} \left(z_0^2(1+\gamma)^2 + 2z_0(1+\gamma) \left(\frac{h_s^2}{2z_0} + \frac{\gamma h_r^2}{2z_0}\right) + \left(\frac{h_s^2}{2z_0} + \frac{\gamma h_r^2}{2z_0}\right)^2 \right) - z_0^2, \quad (\text{B-9})$$

$$h_{e_{z_0 \rightarrow \infty}}^2 = \frac{z_0^2(1+\gamma)^2}{(1+\gamma)^2} + 2z_0 \frac{(1+\gamma)}{(1+\gamma)^2} \left(\frac{h_s^2}{2z_0} + \frac{\gamma h_r^2}{2z_0} \right) + \frac{1}{(1+\gamma)^2} \left(\frac{h_s^2}{2z_0} + \frac{\gamma h_r^2}{2z_0} \right)^2 - z_0^2, \quad (\text{B-10})$$

$$h_{e_{z_0 \rightarrow \infty}}^2 = z_0^2 + \frac{1}{(1+\gamma)} (h_s^2 + \gamma h_r^2) + \frac{1}{(1+\gamma)^2} \left(\frac{h_s^2}{2z_0} + \frac{\gamma h_r^2}{2z_0} \right)^2 - z_0^2, \quad (\text{B-11})$$

and finally

$$h_{e_{z_0 \rightarrow \infty}}^2 = \frac{(h_s^2 + \gamma h_r^2)}{(1+\gamma)}. \quad (\text{B-12})$$

APPENDIX C

We desire to find the depth z_f for a given traveltme error τ . Starting with equations (33) and (34), τ

$$\tau = \frac{1}{V_p} \sqrt{z_0^2 + h_s^2} + \frac{1}{V_s} \sqrt{z_0^2 + h_r^2} - \frac{1}{V_c} \sqrt{z_0^2 + h_s^2} - \frac{1}{V_c} \sqrt{z_0^2 + h_r^2}, \quad (\text{C-1})$$

then

$$V_p \tau = \sqrt{z_0^2 + h_s^2} + \gamma \sqrt{z_0^2 + h_r^2} - \frac{1+\gamma}{2} \sqrt{z_0^2 + h_s^2} - \frac{1+\gamma}{2} \sqrt{z_0^2 + h_r^2}, \quad (\text{C-2})$$

this is simplified to

$$\sqrt{z_0^2 + h_s^2} - \sqrt{z_0^2 + h_r^2} = \frac{2V_p \tau}{1-\gamma}. \quad (\text{C-3})$$

Let

$$k_1 = \frac{2V_p \tau}{1-\gamma}, \quad (\text{C-4})$$

then squaring equation (C-3) we get

$$z_0^2 + h_s^2 + z_0^2 + h_r^2 - 2\sqrt{z_0^2 + h_s^2} \sqrt{z_0^2 + h_r^2} = k_1^2, \quad (\text{C-5})$$

then

$$2\sqrt{z_0^2 + h_s^2} \sqrt{z_0^2 + h_r^2} = 2z_0^2 + h_s^2 + h_r^2 - k_1^2. \quad (\text{C-6})$$

Let

$$k_2^2 = h_s^2 + h_r^2, \quad (\text{C-7})$$

$$k_3^2 = k_2^2 - k_1^2, \quad (\text{C-8})$$

giving

$$4(z_0^2 + h_s^2)(z_0^2 + h_r^2) = 4z_0^4 + k_3^4 + 4z_0^2 k_3^2, \quad (\text{C-9})$$

$$4z_0^2(h_s^2 + h_r^2) + 4h_s^2 h_r^2 = k_3^4 + 4z_0^2 k_3^2, \quad (\text{C-10})$$

and finally

$$z_0^2 = \frac{k_3^4 - 4h_s^2 h_r^2}{4k_2^2 - 4k_3^2}. \quad (\text{C-11})$$

Using only k_l we have

$$z_0^2 = \frac{(h_s^2 + h_r^2 - k_1^2)^2 - 4h_s^2 h_r^2}{4k_1^2}. \quad (\text{C-12})$$